

Magnetized tori around Kerr black holes: analytic solutions with a toroidal magnetic field

S. S. Komissarov[★]

Department of Applied Mathematics, The University of Leeds, Leeds LS2 9GT

Accepted 2006 February 9. Received 2006 February 8; in original form 2006 January 17

ABSTRACT

The dynamics of accretion discs around galactic and extragalactic black holes may be influenced by their magnetic field. In this paper, we generalize the fully relativistic theory of stationary axisymmetric tori in Kerr metric of Abramowicz, Jaroszynski & Sikora by including strong toroidal magnetic field and construct analytic solutions for barotropic tori with constant angular momentum. This development is particularly important for the general relativistic computational magnetohydrodynamics that suffers from the lack of exact analytic solutions that are needed to test computer codes.

Key words: accretion, accretion discs – black hole physics – MHD – methods: analytical – methods: numerical.

1 INTRODUCTION

Accretion discs of black holes have been a subject of intensive observational and theoretical studies for decades. In most of the studies, the discs are treated as purely fluid flows (Shakura & Sunyaev 1974; Fishbone & Moncrief 1976; Abramowicz et al. 1978; Rees et al. 1982). That is, their magnetic fields are considered as dynamically weak and not important for the force balance determining the disc structure. On the other hand, it has long been recognized that magnetohydrodynamics (MHD) turbulence may hold the key to the nature of the disc viscosity that enables the inflow of matter into the black hole (Shakura & Sunyaev 1974). This expectation was confirmed with the discovery of the magnetorotational instability (Balbus & Hawley 1991) that has now become one of the major topics in theoretical and numerical studies of accretion discs. In the simulations of radiatively inefficient discs, they remain relatively weakly magnetized with the magnetization parameter $\beta = (\text{gas pressure})/(\text{magnetic pressure}) \simeq 10\text{--}100$ within the main body of the disc and rising up to $\beta \simeq 1$ only near its inner edge and in the plunging region (Hirose et al. 2004; McKinney & Gammie 2004). However, cooling accretion flows may well evolve towards the state with $\beta < 1$ where the vertical balance against the gravitational force of the central object is achieved by means of magnetic pressure alone (Pariev, Blackman & Boldyrev 2003; Machida, Nakamura & Matsumoto 2006).

On the other hand, there is a general consensus that dynamically strong, ordered, poloidal magnetic field is required both for acceleration and collimation of the relativistic jets that are often produced by the astrophysical black hole–accretion disc systems. Such magnetic field is a key ingredient both in the models where the jet is

powered by the black hole (Blandford & Znajek 1977) and in the models where it is powered by the accretion disc (Bisnovatyi-Kogan & Ruzmaikin 1976; Blandford & Payne 1982). The origin of this field is not very clear. The most popular idea is that it is carried into central parts of the disc–hole system by the accreting flow itself and that the net magnetic flux gradually builds up there during the long-term evolution of the system (Bisnovatyi-Kogan & Ruzmaikin 1976; Thorne & Macdonald 1982). This is more or less what is observed in recent numerical simulations of radiatively inefficient discs with initially weak poloidal field, (Hirose et al. 2004; McKinney & Gammie 2004). However, the strength of magnetic field that can be reached in this way is still unclear (e.g. Livio, Ogilvie & Pringle 1999; Spruit & Uzdensky 2005; Meier 2005; McKinney 2005). The most extreme case, where the disc pressure is dominated by ordered poloidal magnetic field is argued by Meier (2005) as a model for the low/hard state of X-ray binaries. Although much weaker magnetic field is required to explain the observed power of quasar jets within the Blandford–Znajek theory, the pressure of poloidal magnetic field still has to be of the same order as the radiative pressure at the inner edge of the radiatively supported accretion discs (Begelman, Blandford & Rees 1984). Bogovalov & Kel’ner (2005) constructed a model of accretion disc where its angular momentum is carried away by a magnetized wind alone and the inflow of matter and magnetic field is driven entirely by the magnetic torque applied to the disc by the wind. These and other results show that the structure of accretion discs with dynamically strong ordered magnetic fields is a matter of significant astrophysical interest.

General steady-state axisymmetric magnetized discs are described by a very complex equation of the Grad–Shafranov type which does not allow general analytic solutions (Lovelace et al. 1986). However, the equilibrium models with pure azimuthal (toroidal) fields are much simpler and can be constructed using the approach developed for unmagnetized discs (Abramowicz et al.

[★]E-mail: sergei@maths.leeds.ac.uk

1978; Kozłowski, Jaroszynski & Abramowicz 1978). In fact, the predominant motion in accretion discs is a differential rotation and one would expect the azimuthal magnetic field to dominate in the interior of such discs.

Okada, Fukue & Matsumoto (1989) constructed a particular exact solution for the problem of equilibrium torus with purely azimuthal magnetic field. In their approach the Paczynsky & Wiita (1980) potential is utilized to introduce the black hole gravity and the flow dynamics is described by the non-relativistic equations. Although this approach seems to work fine in the case of non-rotating black holes, it is no longer satisfactory in the astrophysically important case of a rapidly rotating black hole where full relativistic treatment is required. In this paper, we develop the general relativistic theory of magnetized tori around rotating black holes. Our analysis closely follows that of Kozłowski et al. (1978) and Abramowicz et al. (1978), including the notation.

Even if tori with dynamically strong magnetic fields do not exist in nature the exact solutions presented here can still be useful for numerical general relativistic MHD (GRMHD), which has attracted a lot of interest recently (Koide, Shibata & Kudoh 1999; Komissarov 2001; De Villiers & Hawley 2003; Gammie, McKinney & Toth 2003; Komissarov 2004; Duez et al. 2005; Anton et al. 2006). One of the problems with general relativistic computational MHD is the lack of exact analytic and semi-analytic solutions that could be used to verify computer codes. The current list of such solutions includes (1) the spherical accretion onto a non-rotating black hole with monopole magnetic field where the magnetic field is dynamically passive (Koide et al. 1999), (2) the perturbative force-free solution of Blandford & Znajek (1977), where both the pressure and the inertia of matter is neglected and the black hole rotates slowly and (3) the so-called Gammie flow, which is a 1D solution of the Weber–Davis type that applies only to the equatorial plane of a black hole (Gammie 1999). One may also try to utilize the axisymmetric semi-analytic self-similar solutions constructed recently by Meliani et al. (2005) but those apply only along the symmetry axis. Obviously, the magnetized torus solution is a very welcome addition to this scarce list. In fact, it is the only solution that is not only (i) fully multidimensional and (ii) involves dynamically important magnetic field, but also (iii) applies in the case of a rapidly rotating black hole. In fact, we have already used this solution to test the 2D GRMHD codes described in Komissarov (2001, 2004).

Throughout this paper, we use the relativistic units where $c = G = M = 1$ and $(-+++)$ signature for the space–time geometry. Following Anile (1989), the magnetic field is rescaled in such a way that the factor 4π disappears from the equations of relativistic MHD.

2 BASIC EQUATIONS

The covariant equations of ideal relativistic MHD are

$$\nabla_\alpha T^{\alpha\beta} = 0, \quad (1)$$

$$\nabla_\alpha {}^*F^{\alpha\beta} = 0, \quad (2)$$

$$\nabla_\alpha \rho u^\alpha = 0, \quad (3)$$

where

$$T^{\alpha\beta} = (w + b^2)u^\alpha u^\beta + \left(p + \frac{1}{2}b^2\right)g^{\alpha\beta} - b^\alpha b^\beta \quad (4)$$

is the energy–momentum tensor, w , p and u^α are the fluid enthalpy, pressure and four-velocity of plasma, respectively, and $g_{\alpha\beta}$ is the

metric tensor (Dixon 1978; Anile 1989).

$${}^*F^{\alpha\beta} = b^\alpha u^\beta - b^\beta u^\alpha \quad (5)$$

is the Faraday tensor and b^α is the four-vector of magnetic field. In the fluid frame $b^\alpha = (0, \mathbf{B})$, where \mathbf{B} is the usual three-vector of magnetic field as measured in this frame, and thus

$$u^\alpha b_\alpha = 0. \quad (6)$$

In the following, we assume that

(i) the space–time is described by the Kerr metric and that $\{t, \phi, r, \theta\}$ are either Kerr–Schild or Boyer–Lindquist coordinates, so that

$$g_{\mu\nu,t} = g_{\mu\nu,\phi} = 0; \quad (7)$$

(ii) the flow is both stationary and axisymmetric, so that

$$f_{,t} = f_{,\phi} = 0, \quad (8)$$

for any physical parameter f ;

(iii) the flow is a pure rotation around the black hole, that is,

$$u^r = u^\theta = 0; \text{ and} \quad (9)$$

(iv) the magnetic field is purely azimuthal, that is,

$$b^r = b^\theta = 0. \quad (10)$$

In terms of partial derivatives, the continuity equation reads

$$(\sqrt{-g}\rho u^v)_{,v} = 0,$$

where g is the determinant of the metric tensor. Given the symmetry conditions (7) and (8), this equation reduces to

$$(\sqrt{-g}\rho u^i)_{,i} = 0,$$

where here and throughout the whole paper $i = r, \theta$. Finally, the condition (9) tells us that this equation is always satisfied.

Since the Faraday tensor is antisymmetric, one may reduce the Faraday equation to

$$(\sqrt{-g}{}^*F^{\mu\nu})_{,\nu} = 0.$$

It is easy to see that this equation is also automatically satisfied given the conditions (7)–(10).

Thus, the only non-trivial results follow from the energy–momentum equation (1). Contracting this equation with the projection tensor $h^\alpha_\beta = \delta^\alpha_\beta + u^\alpha u_\beta$, we obtain

$$(w + b^2)u_\nu u^\nu_{,i} + \left(p + \frac{b^2}{2}\right)_{,i} - b_\nu b^\nu_{,i} = 0. \quad (11)$$

In terms of the angular velocity

$$\Omega = \frac{u^\phi}{u^t} \quad (12)$$

and the specific angular momentum

$$l = \frac{-u_\phi}{u_t} \quad (13)$$

(both u_t and u_ϕ are constants of geodesic motion), this equation reads

$$(\ln |u_t|)_{,i} - \frac{\Omega}{1 - l\Omega} l_{,i} + \frac{p_{,i}}{w} + \frac{(\mathcal{L}b^2)_{,i}}{2\mathcal{L}w} = 0, \quad (14)$$

where

$$\mathcal{L}(r, \theta) = g_{t\phi}g_{t\phi} - g_{t\theta}g_{\theta\phi}. \quad (15)$$

When $b^2 \rightarrow 0$, equation (14) reduces to equation (7) in Abramowicz et al. (1978), which describes equilibrium non-magnetic tori. Thus,

the Lorentz force vanishes and we have a force-free magnetic torus, provided

$$\mathcal{L}b^2 = \text{constant}.$$

Far away from the black hole $g_{t\phi} \rightarrow 0$, $g_{\phi\phi} \rightarrow r^2 \sin^2\theta$, $g_{tt} \rightarrow -1$ and this equation reduces to the familiar

$$B^\phi = \frac{\text{constant}}{r \sin\theta}.$$

3 INTEGRABILITY CONDITIONS

For a barotropic equation of state, where

$$w = w(p), \quad (16)$$

equation (14) leads to

$$d \left(\ln |u_t| + \int_0^p \frac{dp}{w} \right) = \frac{\Omega}{1 - l\Omega} dl - \frac{d(\mathcal{L}b^2)}{2\mathcal{L}w}. \quad (17)$$

In the case of a non-magnetic torus, this equation implies that

$$\Omega = \Omega(l) \quad (18)$$

and thus the surfaces of equal Ω , l , p and ρ coincide (Abramowicz 1971; Abramowicz et al. 1978). Obviously, this does not have to be the case for magnetized tori. If, however, we still assume that $\Omega = \Omega(l)$ then equation (17) can be written as

$$d \left(\ln |u_t| + \int_0^p \frac{dp}{w} - \int_0^l \frac{\Omega dl}{1 - l\Omega} \right) = -\frac{d(\mathcal{L}b^2)}{2\mathcal{L}w}, \quad (19)$$

which implies that the expression of the right-hand side is a total differential. Hence,

$$\tilde{w} = \tilde{w}(\tilde{p}_m), \quad (20)$$

where $\tilde{w} = \mathcal{L}w$ and $\tilde{p}_m = \mathcal{L}p_m$, where $p_m = b^2/2$ is the magnetic pressure, and equation (19) integrates to give

$$\ln |u_t| + \int_0^p \frac{dp}{w} - \int_0^l \frac{\Omega dl}{1 - l\Omega} + \int_0^{\tilde{p}_m} \frac{d\tilde{p}_m}{\tilde{w}} = \text{constant}. \quad (21)$$

Assuming that on the surface of the disc, and hence on its inner edge,

$$p = p_m = 0, \quad u_t = u_{t_{\text{in}}}, \quad l = l_{\text{in}}, \quad (22)$$

one finds the constant of integration as

$$\text{constant} = \ln |u_{t_{\text{in}}}| - \int_0^{l_{\text{in}}} \frac{\Omega dl}{1 - l\Omega}. \quad (23)$$

Following Abramowicz et al. (1978), we introduce the total potential, W , via

$$W = \ln |u_t| + \int_l^{l_\infty} \frac{\Omega dl}{1 - l\Omega}, \quad (24)$$

where l_∞ is the angular momentum at infinity. Provided that l_∞ is finite, we have $u_{t_\infty} = -1$ and $W_\infty = 0$. Using the total potential we can rewrite equation (21) as

$$W - W_{\text{in}} + \int_0^p \frac{dp}{w} + \int_0^{\tilde{p}_m} \frac{d\tilde{p}_m}{\tilde{w}} = 0. \quad (25)$$

With exception for the last term, this equation is the same as equation (9) in Abramowicz et al. (1978) and equation (24) in Kozłowski et al. (1978).

4 BAROTROPIC TORI WITH CONSTANT ANGULAR MOMENTUM

4.1 Theory

Here, we adopt particular relationships $w = w(p)$, $\Omega = \Omega(l)$ and $\tilde{w} = \tilde{w}(\tilde{p}_m)$ that allow one to express the integrals of equation (25) in terms of elementary functions. Namely, we assume that

$$l = l_0, \quad (26)$$

$$p = Kw^\kappa, \quad (27)$$

$$\tilde{p}_m = K_m \tilde{w}^\eta. \quad (28)$$

The last equation can also be written as

$$p_m = K_m \mathcal{L}^{\eta-1} w^\eta. \quad (29)$$

Then equation (25) reduces to

$$W - W_{\text{in}} + \frac{\kappa}{\kappa - 1} \frac{p}{w} + \frac{\eta}{\eta - 1} \frac{p_m}{w} = 0, \quad (30)$$

where

$$W = \ln |u_t|. \quad (31)$$

The obvious parameters of the model are κ , η , l_0 and W_{in} . Two more parameters are needed. We chose these to be the enthalpy, w_c , and the magnetization parameter $\beta_c = (p/p_m)_c$ at the disc centre, $r = r_c$. Following Abramowicz et al. (1978), we define the disc centre as one of the two points in the equatorial plane where l_0 equals to the Keplerian angular momentum

$$l_k = \frac{\pm(r^2 \mp 2ar^{1/2} + a^2)}{r^{3/2} - 2r^{1/2} \pm a}, \quad (32)$$

where the upper sign is used if $l_0 > 0$ and the lower sign otherwise (Bardeen, Press & Teukolsky 1972). The second point is the disc ‘cusp’, $r_{\text{cusp}} < r_c$ (Abramowicz et al. 1978). There exist a number of obvious constraints on the values of these parameters.

In order to avoid divergence of the second and/or the fourth terms in (30) at the disc surface, one should have

$$\kappa, \beta > 1.$$

Under this condition, the disc surface is fully determined by the choice of W_{in} and does not depend on the disc magnetization. This property has already been noticed in Okada et al. (1989).

Only if

$$|l_0| > |l_{ms}|,$$

where l_{ms} is the radius of the marginally stable Keplerian orbit (Bardeen et al. 1972), is the disc detached from the event horizon (Abramowicz et al. 1978). (Solutions attached to the event horizon are improper because they diverge at the event horizon and cannot be continued through it.) The value of l_0 determines the total potential which can be written as

$$W(r, \theta) = \frac{1}{2} \ln \left| \frac{\mathcal{L}}{\mathcal{A}} \right|, \quad (33)$$

where

$$\mathcal{L} = g_{t\phi}g_{t\phi} - g_{tt}g_{\phi\phi}$$

and

$$\mathcal{A} = g_{\phi\phi} + 2l_0g_{t\phi} + l_0^2g_{tt}$$

(see equation A10).

If $|l_0| \geq |l_{mb}|$ then the disc has finite outer radius only for

$$W_{in} < 0.$$

If $|l_{ms}| < |l_0| < |l_{mb}|$, where l_{mb} is the angular momentum of the marginally bound Keplerian orbit (Bardeen et al. 1972), then the disc remains detached from the black hole only if

$$W_{in} \leq W_{cusp},$$

where W_{cusp} is the value of the total potential at the cusp (Abramowicz et al. 1978).

From equation (30), one finds the gas pressure

$$p_c = w_c(W_{in} - W_c) \left(\frac{\kappa}{\kappa - 1} + \frac{\eta}{\eta - 1} \frac{1}{\beta_c} \right)^{-1}, \quad (34)$$

and then the magnetic pressure

$$p_{m_c} = p_c / \beta_c \quad (35)$$

at the disc centre. Using these, one finds the constants K and K_m of the barotropics (equations 27 and 29).

Now one can compute the solution at any location inside the disc. Given the coordinates (r, θ) one computes the potential W using equation (33). If $W < W_{in}$ then this point is inside the disc. The next step is to find the enthalpy, w , as a solution of equation (30). Once w is found one can find p and p_m from equations (27) and (29). The four-velocity vector, $u^\nu = (u^t, u^\phi, 0, 0)$, is given by

$$u^t = -\frac{1}{u_r(1 - l_0\Omega)}, \quad u^\phi = \Omega u^t,$$

where Ω can be found via

$$\Omega = -\frac{g_{t\phi} + g_{tt}l_0}{g_{\phi\phi} + g_{t\phi}l_0}$$

(see Appendix A). The four-vector of magnetic field, $b^\nu = (b^t, b^\phi, 0, 0)$, is given by

$$b^\phi = \pm \sqrt{\frac{2p_m}{\mathcal{A}}}, \quad b^t = l_0 b^\phi$$

(see equation A16).

4.2 Simulations

In order to illustrate the usefulness of this solution for testing GRMHD computer codes, we constructed two equilibrium models and used them to set up the initial solution for 2D axisymmetric simulations using the code described in Komissarov (2004). In both models, the black hole has specific angular momentum $a = 0.9$ which gives $r_{mb} = 1.73$, $r_{ms} = 2.32$, $l_{mb} = 2.63$ and $l_{ms} = 2.49$. In both cases, we used the same value for the barotropic powers κ , $\eta = 4/3$ and the polytropic equation of state with the same ratio of specific heats, $\gamma = 4/3$. The other parameters are given in Table 1. Notice that $l_0 > l_{mb}$ in model A, whereas in model B one has $l_{ms} < l_0 < l_{mb}$ and this allows accretion through the torus cusp (Abramowicz et al. 1978; Kozłowski et al. 1978).

Initially, the space outside of the tori is filled with a rarefied non-magnetic plasma accreting into the black hole. Its density and

pressure are

$$\rho = 10^{-3} \rho_c \exp\left(\frac{-3r}{r_c}\right), \quad p = K \rho^\kappa.$$

Its velocity in the frame of local fiducial observer (FIDO; Thorne & Macdonald 1982) is radial and has the magnitude

$$v = \beta^{\hat{r}} \left[1 - \left(\frac{r_g}{r} \right)^4 \right],$$

where $\beta^{\hat{r}}$ is the radial component of velocity of the spatial grid relative to FIDO. This introduces inflow through the horizon with the local velocity of FIDOs and at the same time allows only small poloidal velocity jumps at the torus surface. The latter property allows to avoid strong rarefactions that may originate at the torus surface right at the start of simulations. The initial distributions of ρ , Ω and β for the model A, which is a more extreme case, are shown in Fig. 1. Model B appears very similar.

In these simulations, we utilized the Kerr–Schild coordinates (r, θ) . The computational domain is $[1.35, 53.3] \times [0, \pi]$ with 320 cells in each direction. At lower resolution the effects of numerical diffusion become rather noticeable. The grid is uniform in the θ -direction and the cell size in the radial direction is such that in the equatorial plane $g_{\theta\theta} \Delta\theta^2 = g_{rr} \Delta r^2$. This ensures that computational cells have approximately equal lengths in both directions and throughout the whole grid.

The rotational period of the disc centre is rather long; $\tau_r = 68$ in model A and $\tau_r = 45$ in model B. However, the dynamical time-scale, τ_d , for the disc centre is significantly shorter. Indeed, in both of these models the fast magnetosonic speed in the disc centre is $a_f \simeq 0.18$, whereas the length-scale of pressure distribution at this location is $L_c \simeq 1.0$. This gives the dynamical time-scale $\tau_d \simeq 6$. Since it is the dynamical time-scale that determines how quickly the system reacts to perturbations of its equilibrium state, it is quite sufficient to carry out simulations for only $t = \text{few } \tau_d$ in order to test the ability of our numerical code to correctly reproduce these equilibrium solutions. In order to demonstrate this, we have carried out test simulations for model A not only with our ‘proper code’ but also with its two corrupted versions. In the first version, it is only the electromagnetic pressure, $(B^2 + E^2)/2$, that was taken into account in the calculations of the Maxwell stress tensor. In the second and more drastic version, we omitted all the contributions of the electromagnetic field to the stress–energy–momentum tensor. The results are presented in Fig. 2. One can see that already at $t \simeq 2\tau_d$, the solutions obtained with the corrupted versions are significantly different from the initial equilibrium solution. With the second corrupted version, the disc simply collapses towards the equator due to the lack of magnetic support against gravity.

Fig. 2 also presents the proper numerical solution at $t = 200$, which is 30–40 times larger than τ_d . ‘Naked-eye’ inspection shows that this solution is very similar to the initial equilibrium one that is presented in Fig. 1. This is confirmed by the 1D density plots showing in details the distributions along and across the symmetry plane: Fig. 3 for model A and Fig. 4 for model B. Other images also reveal what appears to be surface waves propagating away from the black hole and becoming noticeable in the more remote parts of the tori.

5 SUMMARY

In this paper, we have generalized the relativistic theory of thick accretion discs around Kerr black holes (Fishbone & Moncrief 1976;

Table 1. Parameters of the models used for test simulations.

Model	l_0	r_{cusp}	r_c	W_{cusp}	W_c	W_{in}	β_c
A	2.8	1.58	4.62	0.702	−0.103	−0.030	0.1
B	2.6	1.78	3.40	−0.053	−0.136	−0.053	1.0

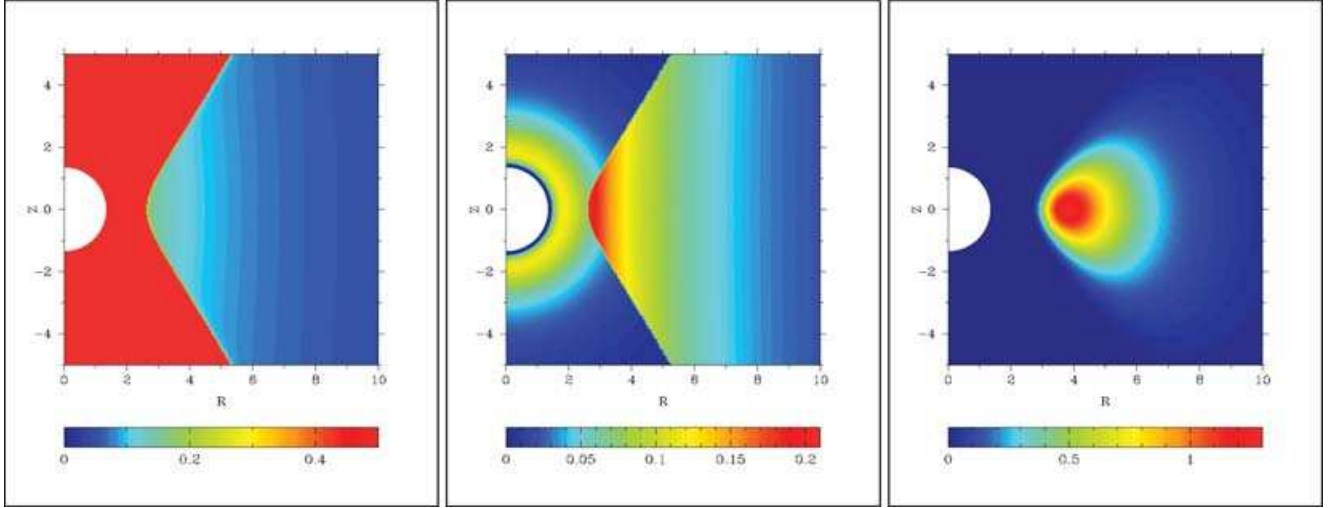


Figure 1. Exact solution for model A. The horizontal coordinate is $R = r \sin \theta$ and the vertical coordinate is $Z = r \cos \theta$. Left-hand panel: β , middle panel: Ω , right-hand panel: ρ .

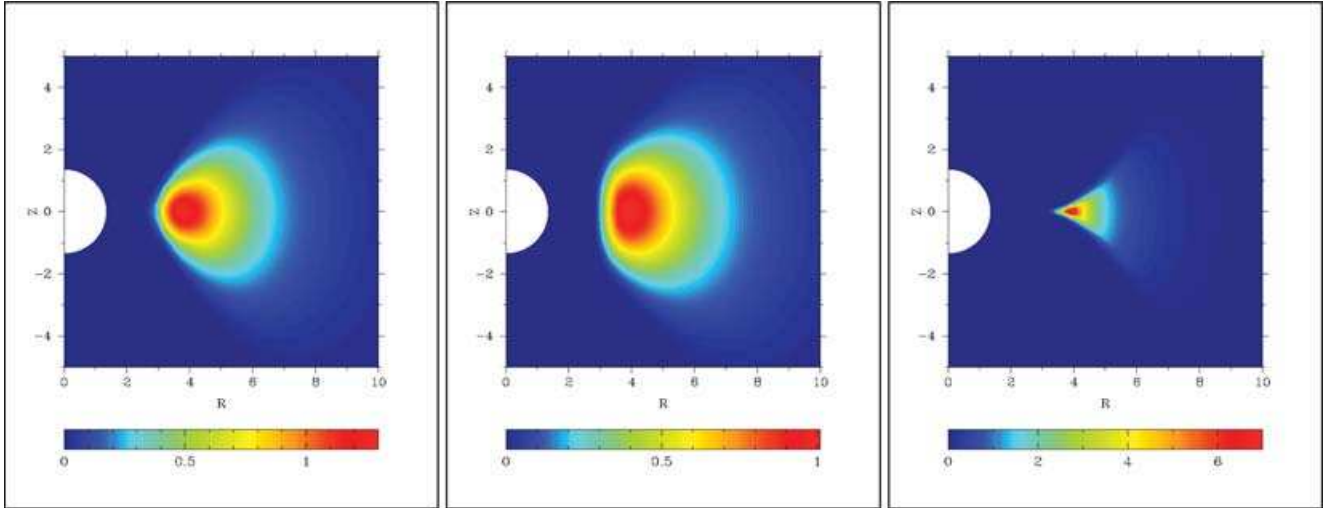


Figure 2. The density distributions for the model A obtained with our actual numerical code and its corrupted versions. In all these plots the linear scaling is used. Left-hand panel: the solution obtained with the uncorrupted code at $t = 200$. Middle panel: the solution obtained with the corrupted version of the code at $t = 14$. Here, we retained only the contribution of magnetic pressure in the Maxwell stress tensor. Right-hand panel: the solution obtained with the corrupted version of the code at $t = 14$. Here, all the electromagnetic contributions to the stress-energy-momentum tensor were omitted.

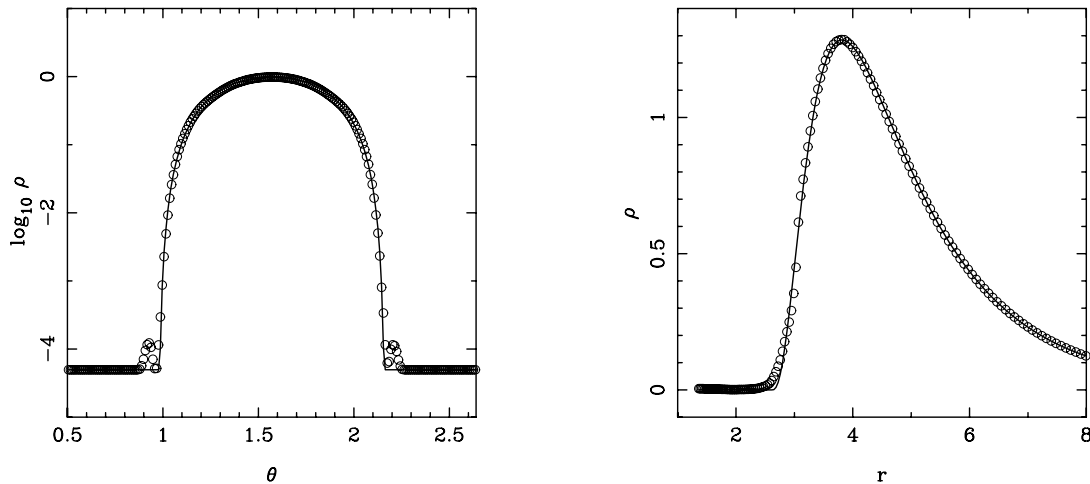


Figure 3. Density distribution at $t = 60$ for model A. The solid lines show the exact equilibrium solution. Left-hand panel: $\log_{10} \rho$ against polar angle θ at $r = r_c$, the disc centre location. Right-hand panel: ρ against r in the equatorial plane.

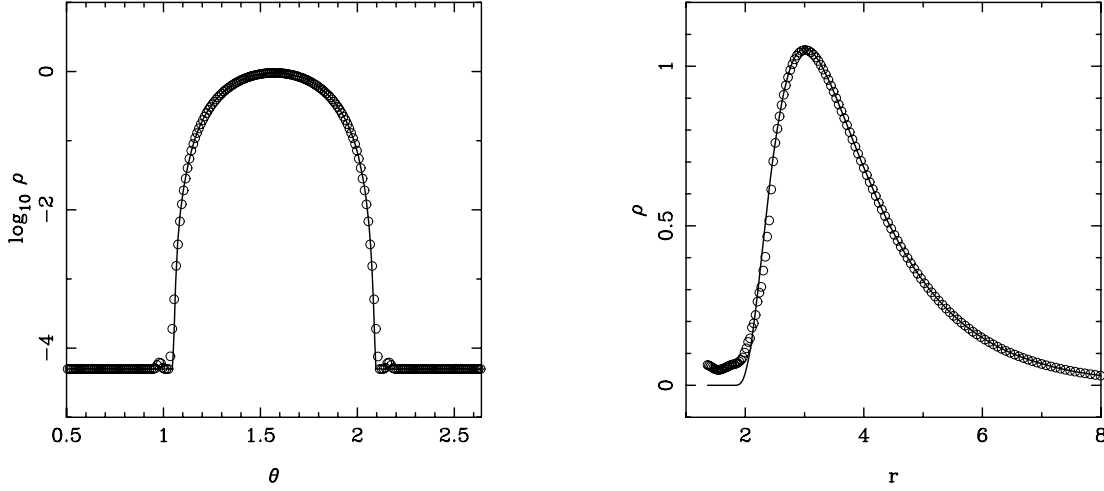


Figure 4. Density distribution at $t = 60$ for model B. The solid lines show the exact equilibrium solution. Left-hand panel: $\log_{10} \rho$ against the polar angle θ at $r = r_c$, the disc centre location. Right-hand panel: ρ against r in the equatorial plane.

Abramowicz et al. 1978; Kozłowski et al. 1978) by including dynamically strong toroidal (azimuthal) magnetic field. As expected, this inclusion of magnetic field leads to a whole new class of equilibrium solutions that differ in strength and spatial distribution of the field. In particular, we have described the way of constructing barotropic tori with constant angular momentum – under such conditions, the differential equations of magnetostatics are easily integrated and reduce to simple algebraic equations.

By now, it has become clear that magnetic field plays many important roles in the dynamics of astrophysical black hole–accretion disc systems. However, the structure of this field may be more complex than just azimuthal loops and as a result the analytic solutions constructed in this paper may turn out not to be particularly suitable for modelling real astrophysical objects. Even so they will certainly be helpful in testing computer codes for general relativistic MHD that are becoming invaluable tools in the astrophysics of black holes–accretion discs.

ACKNOWLEDGMENT

This research was funded by PPARC under the rolling grant ‘Theoretical Astrophysics in Leeds’.

REFERENCES

- Abramowicz M., 1971, *Acta Astron.*, 21, 81
 Abramowicz M., Jaroszynski M., Sikora M., 1978, *A&A*, 63, 221
 Anile A. M., 1989, *Relativistic Fluids and Magneto-Fluids*. Cambridge Univ. Press, Cambridge
 Anton L., Zanotti O., Miralles J. A., Martí J. M., Ibanez J. M., Font J. A., Pons J. A., 2006, *ApJ*, 637, 296.
 Balbus S. A., Hawley J. F., 1991, *ApJ*, 376, 214
 Bardeen J. M., Press W. H., Teukolsky S. A., 1972, *ApJ*, 178, 347
 Begelman M. C., Blandford R. D., Rees M. J., 1984, *Rev. Mod. Phys.*, 56, 255
 Bisnovatyi-Kogan G. S., Ruzmaikin A. A., 1976, *Ap&SS*, 42, 401
 Blandford R. D., Payne D. G., 1982, *MNRAS*, 199, 883
 Blandford R. D., Znajek R. L., 1977, *MNRAS*, 179, 433
 Bogovalov S. V., Kel’ner S. R., 2005, *Astron. Rep.*, 49, 57
 De Villiers J., Hawley J. F., 2003, *ApJ*, 589, 458
 Dixon G., 1978, *Special Relativity, the Foundation of Macroscopic Physics*. Cambridge Univ. Press, Cambridge

- Duez M. D., Liu Y. T., Shapiro S. L., Stephens B. C., 2005, *Phys. Rev. D*, 72, 024028
 Fishbone L. G., Moncrief V., 1976, *ApJ*, 207, 962
 Gammie C. F., 1999, *ApJ*, 522, L57
 Gammie C. F., McKinney J. C., Toth G., 2003, *ApJ*, 589, 444
 Hirose S., Krolik J. H., De Villiers J.-P., Hawley J. F., 2004, *ApJ*, 606, 1083
 Koide S., Shibata K., Kudoh T., 1999, *ApJ*, 522, 727
 Komissarov S. S., 2004, *MNRAS*, 350, 1431
 Komissarov S. S., 2001, in Toro E. F., ed., *Godunov Methods: Theory and Applications*. Kluwer, New York, p. 519
 Kozłowski M., Jaroszynski M., Abramowicz M., 1978, *A&A*, 63, 209
 Livio M., Ogilvie G., Pringle J. E., 1999, *ApJ*, 512, 100
 Lovelace R. V. E., Mehanian C., Mobarri C. M., Sulkanen M. E., 1986, *ApJS*, 62, 1
 Machida M., Nakamura K., Matsumoto R., 2006, *PASJ*, in press
 McKinney J. C., 2005, *ApJ*, 630, L5
 McKinney J. C., Gammie C. F., 2004, *ApJ*, 611, 977
 Meier D. L., 2005, *Ap&SS*, 300, 55
 Meliani Z., Sauty C., Vlahakis N., Tsiganos K., Trussoni E., 2006, *A&A*, 447, 797
 Okada R., Fukue J., Matsumoto R., 1989, *PASJ*, 41, 133
 Paczynsky B., Wiita P. J., 1980, *A&A*, 88, 23
 Pariev V. I., Blackman E. G., Boldyrev S. A., 2003, *A&A*, 407, 403
 Rees M. J., Phinney E. S., Begelman M. C., Blandford R. D., 1982, *Nat*, 285, 17
 Shakura N. I., Sunyaev R. A., 1974, *A&A*, 24, 337
 Spruit H. C., Uzdensky D. A., 2005, *ApJ*, 629, 960
 Thorne K. S., Macdonald D. A., 1982, *MNRAS*, 198, 339.
 van Putten M. H. P. M., Ostriker E. C., 2001, *ApJ*, 552, L31

APPENDIX A:

Here, we derive equations (11) and (14) of the main paper.

A1 Equation (11)

The contraction of the energy–momentum equation,

$$\nabla_\alpha T^{\alpha\beta} = 0,$$

with the projection tensor

$$h^\alpha_\beta = \delta^\alpha_\beta + u^\alpha u_\beta$$

leads to

$$h_i^\alpha \nabla_\gamma [(w + b^2) u^\gamma u_\alpha] + h_i^\alpha \nabla_\gamma \left[\left(p + \frac{b^2}{2} \right) \delta_\alpha^\gamma \right] + h_i^\alpha \nabla_\gamma (b^\gamma b_\alpha) = 0, \quad (\text{A1})$$

where $i = r, \theta$. Applying the product rule and using that $h_\beta^\alpha u_\alpha = 0$ and $u^\alpha \nabla_\gamma u_\alpha = 0$, one can write

$$h_i^\alpha \nabla_\gamma [(w + b^2) u^\gamma u_\alpha] = (w + b^2) [\nabla_\gamma (u^\gamma u_i) - u_i \nabla_\gamma u^\gamma].$$

The second term in the square brackets vanishes because of the symmetry conditions (7)–(10). Applying the well-known result for the divergence of a second-rank symmetric tensor, one obtains

$$\nabla_\gamma (u^\gamma u_i) = \frac{1}{\sqrt{-g}} (\sqrt{-g} u^\gamma u_i)_{,\gamma} - \frac{1}{2} g_{\mu\nu,i} u^\mu u^\nu.$$

The first term in this equation vanishes because of the same symmetry conditions whereas

$$g_{\mu\nu,i} u^\mu u^\nu = -2u_i u^v_{,i}.$$

Thus, one has

$$h_i^\alpha \nabla_\gamma [(w + b^2) u^\gamma u_\alpha] = (w + b^2) u_i u^v_{,i}. \quad (\text{A2})$$

Now we deal with the second term in (A1).

$$\begin{aligned} h_i^\alpha \nabla_\gamma \left[\left(p + \frac{b^2}{2} \right) \delta_\alpha^\gamma \right] &= h_i^\alpha \nabla_\gamma \left(p + \frac{b^2}{2} \right) \\ &= \left(p + \frac{b^2}{2} \right)_{,i} + u_i u^\gamma \left(p + \frac{b^2}{2} \right)_{,\gamma}. \end{aligned}$$

The second term on the right-hand side of this equation vanishes because of the symmetries and hence we have

$$h_i^\alpha \nabla_\gamma \left[\left(p + \frac{b^2}{2} \right) \delta_\alpha^\gamma \right] = \left(p + \frac{b^2}{2} \right)_{,i}. \quad (\text{A3})$$

As to the third term in (A1),

$$\begin{aligned} h_i^\alpha \nabla_\gamma (b^\gamma b_\alpha) &= h_i^\alpha \left(\frac{1}{\sqrt{-g}} (\sqrt{-g} b^\gamma b_\alpha)_{,\gamma} - \frac{1}{2} g_{\mu\nu,\alpha} b^\mu b^\nu \right) \\ &= -\frac{1}{2} h_i^\alpha g_{\mu\nu,\alpha} b^\mu b^\nu \\ &= -\frac{1}{2} (g_{\mu\nu,i} b^\mu b^\nu + u_i u^\alpha g_{\mu\nu,\alpha} b^\mu b^\nu) \\ &= -\frac{1}{2} g_{\mu\nu,i} b^\mu b^\nu \\ &= -\frac{1}{2} (b^2_{,i} - 2b_i b^v_{,i}). \end{aligned} \quad (\text{A4})$$

During this reduction, we twice used the symmetry conditions. Substituting of results (A2)–(A4) into equation (A1) leads to

$$(w + b^2) u_i u^v_{,i} + \left(p + \frac{b^2}{2} \right)_{,i} - b_i b^v_{,i} = 0, \quad (\text{A5})$$

which is equation (11) of the main paper.

A2 Equation (14)

From the definitions of the angular velocity, Ω , the angular momentum, l , and the symmetries of the problem, it immediately follows that

$$l = -\frac{g_{t\phi} + g_{\phi\phi}\Omega}{g_{tt} + g_{t\phi}\Omega}, \quad (\text{A6})$$

$$\Omega = -\frac{g_{t\phi} + g_{tt}l}{g_{\phi\phi} + g_{t\phi}l}, \quad (\text{A7})$$

where we assumed the Kerr metric in either Kerr–Schild or Boyer–Lindquist coordinates. From the definition of 4-velocity, it follows that

$$g_{\mu\nu} u^\mu u^\nu = -1.$$

In the case under consideration this leads to

$$(u^t)^2 = -(g_{tt} + 2g_{t\phi}\Omega + g_{\phi\phi}\Omega^2)^{-1} \quad (\text{A8})$$

and

$$u^t u_t = -\frac{1}{1 - l\Omega}. \quad (\text{A9})$$

From equations (A7)–(A9) one finds

$$(u_t)^2 = \frac{\mathcal{L}}{\mathcal{A}}, \quad (\text{A10})$$

where

$$\mathcal{L} = g_{t\phi} g_{t\phi} - g_{tt} g_{\phi\phi} \quad (\text{A11})$$

and

$$\mathcal{A} = g_{\phi\phi} + 2l g_{t\phi} + l^2 g_{tt}. \quad (\text{A12})$$

From the constraint equation (6) and the conditions (9,10) one finds

$$b^t = l b^\phi, \quad (\text{A13})$$

$$b_t = -\Omega b_\phi. \quad (\text{A14})$$

These allow us to write

$$b^2 = b_\phi b^\phi (1 - l\Omega) \quad (\text{A15})$$

and

$$b^2 = (b^\phi)^2 \mathcal{A}. \quad (\text{A16})$$

Now, we reduce the terms $u_i u^v_{,i}$ and $b_i b^v_{,i}$ in equation (A5). Using the definitions of Ω and l , one derives

$$\begin{aligned} u_i u^v_{,i} &= -u^v u_{v,i} \\ &= -u^t u_{t,i} - u^\phi u_{\phi,i} \\ &= -u^t [u_{t,i} - \Omega(l u_t)_{,i}] \\ &= -u^t [u_{t,i} (1 - l\Omega) - \Omega u_t l_{,i}]. \end{aligned}$$

The substitution of u^t from (A9) into the last equation gives us

$$u_i u^v_{,i} = (\ln |u_t|)_{,i} - \frac{\Omega}{1 - l\Omega} l_{,i}. \quad (\text{A17})$$

Using (A13) and (A14), one writes

$$\begin{aligned} b_i b^v_{,i} &= b_t b^t_{,i} + b_\phi b^\phi_{,i} \\ &= -\Omega b_\phi (l b^\phi)_{,i} + b_\phi b^\phi_{,i} \\ &= b_\phi b^\phi_{,i} (1 - l\Omega) - \Omega b_\phi b^\phi l_{,i}. \end{aligned}$$

The substitution of b_ϕ from (A15) into this equation gives

$$b_v b_{,i}^v = b^2 (\ln |b^\phi|)_{,i} - \frac{\Omega b^2}{1 - l\Omega} l_{,i}. \quad (\text{A18})$$

Substituting (A17) and (A18) into (A5), one finds

$$w \left[(\ln |u_t|)_{,i} - \frac{\Omega}{1 - l\Omega} l_{,i} \right] + p_{,i} + b^2 \left(\ln \left| \frac{u_t}{b^\phi} \right| \right)_{,i} + b_{,i}^2 = 0. \quad (\text{A19})$$

Using (A10) and (A16), one obtains

$$b^2 \left(\ln \left| \frac{u_t}{b^\phi} \right| \right)_{,i} + b_{,i}^2 = \frac{(\mathcal{L}b^2)_{,i}}{2\mathcal{L}}.$$

Thus, (A19) can be written as

$$(\ln |u_t|)_{,i} - \frac{\Omega}{1 - l\Omega} l_{,i} + \frac{p_{,i}}{w} + \frac{(\mathcal{L}b^2)_{,i}}{2\mathcal{L}w} = 0, \quad (\text{A20})$$

which is equation (14) of the main paper.

This paper has been typeset from a $\text{\TeX}/\text{\LaTeX}$ file prepared by the author.